The method has been validated using several ECG records from the MIT-BIH arrhythmia database. None of the more complex cases result in sensitivity less than 98.10% and specificity of 100%, even for ECGs with ambiguous waves. These results show that the developed method provides a reliable and accurate detection of the fiducial points. It outperforms the other algorithms and has an average detection accuracy of 99.64% which is well within the acceptable range. In addition, through simple modifications, it would be robust to PQRST variations, which incorporates several pathological conditions. For highly abnormal ECGs, where some of the fiducial points are missing, an experimental decision rule is used. This gives the opportunity to study very low amplitude complexes, and therefore, it is suited for precise ECG fiducial points detection.

REFERENCES

[1] B. U. Köhler, C. Hennig, and R. Orglmeister, "The principles of software QRS detection," *IEEE Eng. Med. Biol. Mag.*, vol. 21, pp. 42–57, Jan.–Feb. 2002.
[2] C. Li, C. Zheng, and C. Tai, "Detection of ECG characteristic points using wavelet transforms," *IEEE Trans. Biomed. Eng.*, vol. 42, no. 1, pp. 21–28, Jan. 1995.
[3] S. Krimi, K. Ouni, and N. Ellouze, "T-Wave detection based on an adjusted wavelet transform modulus maxima," *Int. J. Biomed. Sci.*, vol. 1, pp. 128–132, Feb. 2006.
[4] S. Kadambe, R. Murray, and G. Boudreaux-Bartels, "Wavelet transform-based QRS complex detector," *IEEE Trans. Biomed. Eng.*, vol. 46, no. 7, pp. 838–848, Jul. 1999.
[5] D. B. Keenan, "Detection and correction of ectopic beats for HRV analysis applying discrete wavelet transforms," *Int. J. Inf. Technol.*, vol. 2, pp. 54–60, Jan. 2005.
[6] O. Sayadi and M. B. Shamsollahi, "Multiadaptive bionic wavelet transform: Application to ECG denoising and baseline wandering reduction," in *EURASIP J. Adv. Signal Process.*, 2007, vol. 2007, doi:10.1155/2007/41274.
[7] O. Sayadi and M. B. Shamsollahi, "ECG denoising with adaptive bionic wavelet transform," in *Proc. EMBS*, 2006, pp. 6597–6600.
[8] O. Sayadi and M. B. Shamsollahi, "ECG baseline correction with adaptive bionic wavelet transform," in *Proc. ISSPA*, 2007, pp. 1–4.
[9] P. E. McSharry, G. D. Clifford, L. Tarassenko, and L. A. Smith, "A dynamical model for generating synthetic electrocardiogram signals," *IEEE Trans. Biomed. Eng.*, vol. 50, no. 3, pp. 289–294, Mar. 2003.
[10] P. E. McSharry and G. D. Clifford, ECGSYN -A Realistic ECG Waveform Generator, Dec. 2003 [Online]. Available: http://www.physionet.org/physiotools/ecgsyn/
[11] J. Yao and Y. T. Zhang, "Bionic wavelet transform: A new time-frequency method based on an auditory model," *IEEE Trans. Biomed. Eng.*, vol. 48, no. 8, pp. 856–863, Aug. 2001.
[12] J. Yao and Y. T. Zhang, "The application of bionic wavelet transform to speech signal processing in cochlear implants using neural network simulations," *IEEE Trans. Biomed. Eng.*, vol. 49, no. 11, pp. 1299–1309, Nov. 2001.
[13] G. D. Clifford, A. Shoeb, P. E. McSharry, and B. A. Janz, "Model-based filtering, compression and classification of the ECG," in *Proc. BEM & NFSI*, 2005, pp. 1–4.
[14] M. A. Haque, M. E. Rahman, C. A. A. Sayeed, and B. M. Z. Uddin, "A fast algorithm in detecting ECG characteristic points," *Proc. ICECE*, pp. 160–163, 2002.
[15] R. G. Lee, I. C. Cho1, C. C. Lai, M. H. Liu, and M. J. Chiu, "A novel QRS detection algorithm applied to the analysis for heart rate variability of patients with sleep apnea," *J. Biomed. Eng., Appl., Basis & Commun.*, vol. 17, pp. 258–262, Oct. 2005.
[16] The MIT-BIH Arrhythmia Database May 1997 [Online]. Available: http://physionet.ph.biu.ac.il/physiobank/database/mitdb/
[17] V. X. Afonso, W. J. Tompkins, T. Q. Nguyen, and S. Luo, "ECG beat detection using filter banks," *IEEE Trans. Biomed. Eng.*, vol. 46, no. 2, pp. 192–202, Feb. 1999.

Automated Estimation of the Upper Surface of the Diaphragm in 3-D CT Images

Xiangrong Zhou*, Hiroaki Ninomiya, Takeshi Hara, Hiroshi Fujita, Ryujiro Yokoyama, Huayue Chen, Takuji Kiryu, and Hiroaki Hoshi

Abstract—This communication describes a fully automated method by which the position of the diaphragm surface can be estimated by deforming a thin-plate model to match the bottom surface of the lung in CT images. This method was applied to 338 X-ray CT scans, and its validity was proved by the experimental results.

Index Terms—Computer-aided diagnosis (CAD), diaphragm, segmentation, three-dimensional (3-D) image processing, X-ray torso CT images.

I. BACKGROUND

Modern CT scanners can generate volumetric images with high spatial resolution within 20 to 30 s; these images display the details of the human body. Torso X-ray CT scans are widely used in clinical medicine for lesion detection and surgical operations. However, it is tedious for radiologists to interpret such volumetric images that include over 1000 transverse slices on a monitor or film. Computer-aided diagnosis (CAD) systems that can exhibit the 3-D anatomical structure of the human body and determine the location of suspicious regions are highly expected to reduce the tedium and increase the accuracy of medical image interpretation.

Recognition of the anatomical structures of the human body is the first step in the development of a CAD system. Further, for torso CT images, identification of the diaphragm and the subsequent division of the torso into regions (chest and abdomen) is an important initial step for anatomical structure recognition. Beichel *et al.* proposed a diaphragm surface extraction approach using a semiautomatic process [1]. However, a fully automated process for diaphragm identification and body cavity division is required for the development of a CAD system. In this communication, we propose an automated scheme to locate the upper surface of the diaphragm in noncontrast CT images, and we evaluate its performance by using a large database of torso CT images.

II. METHODS

The diaphragm is located below the lungs and above the liver. The shape of the diaphragm is not uniform and changes with breathing. Moreover, it is composed of muscles that have a similar density (CT

(a) Torso CT images showing only the chest region
(White lines: initial diaphragmatic lung surfaces)

(b) Thin-plate model before deformation

(c) Torso CT images showing chest region only
(White lines: diaphragmatic lung surfaces)

(d) 3-D view of the diaphragmatic lung surfaces

(e) 3-D view of the diaphragm (arrow)

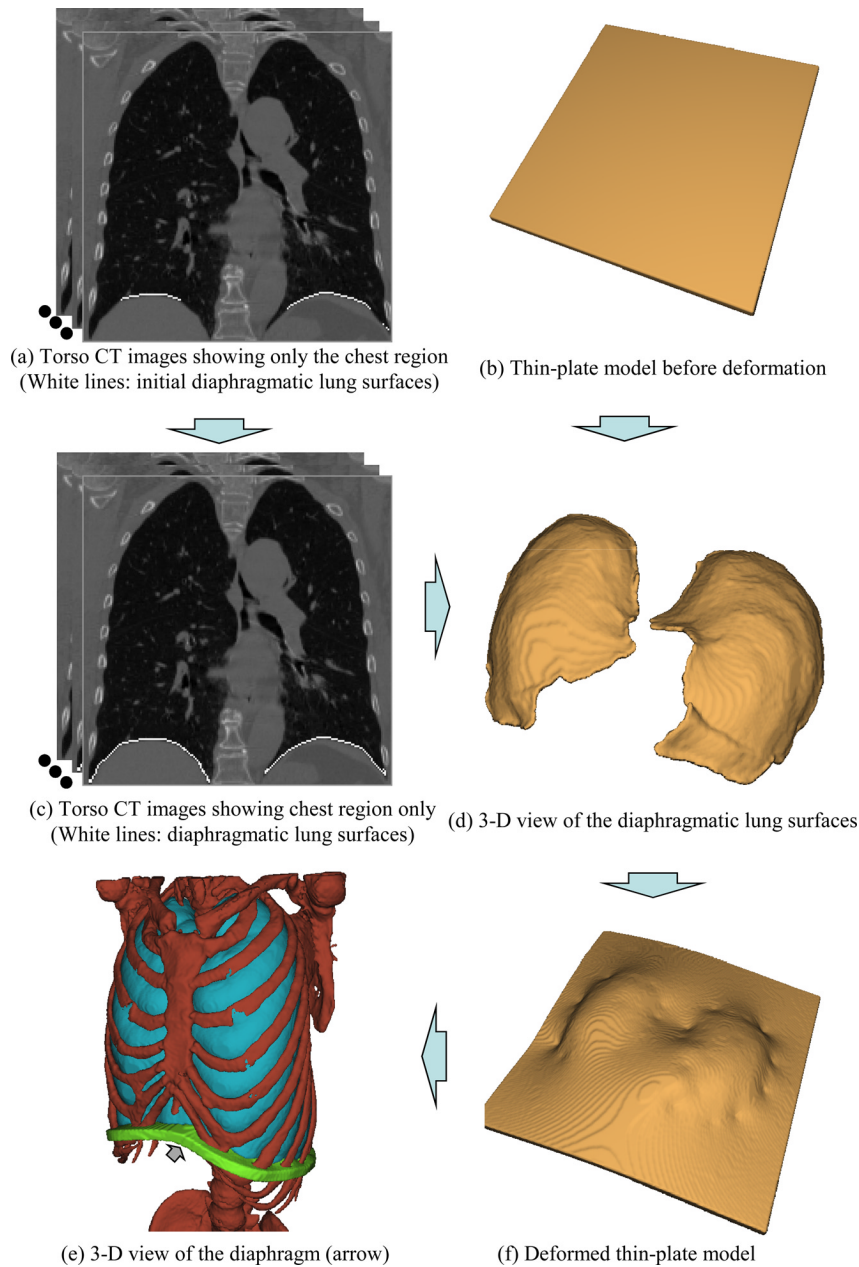(f) Deformed thin-plate model

Fig. 1.   Outline of the automated diaphragm estimation from CT images.

number) distribution as that in surrounding organs such as the liver, heart, and spleen. Thus, it is difficult to identify the diaphragm based on the CT value or its shape. Our proposed method estimates the location and shape of the diaphragm based on the spatial relations between the lung surfaces and the diaphragm; in this technique, a thin-plate model is deformed to fit the bottom surface of the lung (shown in Fig. 1). The process involves the three steps outlined in the following three subsections.

A. Segmentation of the Lung Region

In a torso CT image, the various human tissue regions (a 3-D volumetric matrix) are separated from the background (mainly air) by a gray-level thresholding process. The thresholding value th_{air} is automatically determined by discriminant analysis of the CT number histogram [2]. Among the segmented air regions within the torso, a 3-D connected component with the largest volume is selected as the initial lung region, and it includes the airways of the trachea and the left and

right lung. The airways of the trachea and bronchus are then segmented by a 3-D region growing method [3]. By eliminating the airway region from the initial lung region, the left and right lungs become two isolated regions without any 3-D connections and can be identified based on connected-component labeling and selecting based on their center coordinates and volumes [3].

B. Identification of the Diaphragmatic Lung Surface

The voxels on the lung surfaces are extracted by a 3-D surface tracing process. On each voxel, the normal vector V of the lung surface is calculated. The voxel P on the lung surfaces that satisfies the condition $\{-(3/4)\pi < \text{direction of } V \text{ on } P < -(1/4)\pi\}$ is regarded as the candidate voxel, and the largest connected component of the candidates on the left/right lung surface is considered as the initial left/right diaphragmatic lung surface [Fig. 1(a)]. The region growing method is applied to refine the initial result and identify the final diaphragmatic lung surface [Fig. 1(c)].

C. Estimation of the Position of the Diaphragm

Using a grid with regular intervals (3 mm) on the cross section of the human body, subsample points on the grid are selected from the diaphragmatic surfaces of the lung regions. A thin-plate model [Fig. 1(b)] is deformed to fit the subsample points on the diaphragmatic lung surface [Fig. 1(d)] by using a 3-D thin-plate spline method [4]. The initial thin-plate model is a 3-D binary image $I(x, y, z)$ satisfied the condition

$$\{\text{If } (\text{const}1 < z < \text{const}1 + \text{const}2) \, I(x, y, z) = 1;$$
$$\text{else } I(x, y, z) = 0\}$$

where x, y, z are the spatial coordinate of lateral, anterior, and inferior directions of human body. The deformed thin-plate model [Fig. 1(f)] in the body cavity (extracted using a ball-kernel region growing method [5]) provides the position of the diaphragm [Fig. 1(e)].

III. RESULTS AND DISCUSSION

To estimate the position of the diaphragm, we applied this method to 338 patients (male: 210; female: 128; age: 12–89 years) who underwent torso X-ray CT scans. CT images of each patient were acquired with a multislice CT scanner (UltraSpeed of General Electric) by using a common protocol (120 kV/Auto mA) without the use of any contrast media. Each CT scan covered the entire human torso with approximately 1000 slices, an isotopic spatial resolution of approximately 0.6 mm, and a density (CT number) resolution of 12 bits. The const1 and const2 of thin-plate model were set as 0 and 10. Fig. 1 shows an example of the original CT images and the segmentation result. The mean value of th_{air} in 338 cases was -461.3 HU with a standard deviation of 10.6 after the application of discriminant analysis [2], [3].

The accuracy of the diaphragm extraction was evaluated through two stages by author H. Chen, who is a Medical Doctor specializing in human anatomy with more than ten years' experience. In the first stage, the discrepancy e was estimated by the maximum distance between the extracted surface and the true diaphragm on the CT scans virtually using a graphics user interface that could show the slice-by-slice comparisons of the diaphragm recognition results with the original CT images in three views (sagittal, coronal, and cross-sectional views) and calculate the distance between two points on an image interactively. The results were categorized into two groups: good ($e <= \text{th}$) and poor ($e > \text{th}$) with th fixed at 5 voxels due to a requirement for a CAD system to be subsequently developed. It was found that 78.4% (265/338) of the extractions were good, and 21.6% (73/338) were poor. Some extractions were poor due to the impact of fluid accumulation or inflammation between the diaphragm and the lungs. In the second stage of the accuracy evaluation, the upper surfaces of the diaphragm in 30 patients who were randomly selected from the group rated as good were manually identified (manual sketching the upper surfaces slice-by-slice on CT images and refining its shape in 3-D) by author H. Chen as the ground truth for evaluations. The absolute values of the shortest Euclidian distance between every point on the surface identified by author H. Chen and the surface extracted by the algorithm were measured and an average value was taken as the error in each patient case. The average error over 30 cases was 2.97 voxels, with a standard deviation of 0.99. The computing time of the segmentation process is about 15 min for one CT case using a computer (CPU: AMD Opteron 2.2 GHz). Comparing with the manual identification (1–2 CT cases/1 working day), our automated process could save the doctors a lot of their time and energy.

The state of respiration during the CT scans influenced the shape of the diaphragm in the CT images. Shape model-based segmentation of the diaphragm [1] appeared to be sensitive to the respiration state during the acquisition of the CT images. Instead of using a predefined shape model, we used the bottom surface of the lung to directly determine the shape of the diaphragm in the CT images, and we avoided the influence of the variation in the shape of the diaphragm that is caused by respiration during the CT scan. Naturally, the usefulness of our method is limited to the condition that the lung regions in the CT images are normal.

IV. CONCLUSION

We proposed a fully automated method to estimate the position of the upper surface of the diaphragm from noncontrast torso CT images. This method was applied to 338 torso CT images, and the diaphragm was successfully identified in 265 images. The validity and usefulness of this method was demonstrated. We also confirmed that the results of diaphragm recognition were useful for the identification of the anatomical structure of the body cavity from CT images [5].

REFERENCES

[1] R. Beichel, G. Gotschuli, E. Sorantin, F. Leberl, and M. Sonka, "Diaphragm dome surface segmentation in CT data sets: A 3D active appearance model approach," in *Proc. SPIE Med. Image Process.*, 2002, vol. 4684, pp. 475–484.

[2] N. Otsu, "A threshold selection method from gray-level histograms," *IEEE Syst., Man, Cybern. C*, vol. SMC-9, no. 1, pp. 62–66, 1979.

[3] X. Zhou, T. Hayashi, T. Hara, H. Fujita, R. Yokoyama, T. Kiryu, and H. Hoshi, "Automatic segmentation and recognition of anatomical lung structures from high-resolution chest CT images," *Comput. Med. Imaging Graph.*, vol. 30, no. 5, pp. 299–313, 2006.

[4] F. L. Bookstein, "Principal warps: Thin-Plate splines and the decomposition of deformations," *IEEE Trans. Pattern Anal. Mach. Intell.*, vol. 11, no. 6, pp. 567–585, Jun. 1989.

[5] X. Zhou, T. Hara, H. Fujita, R. Yokoyama, T. Kiryu, M. Kanematsu, and H. Hoshi, "Preliminary study for automated recognition of anatomical structure from torso CT images," in *Proc. 27th. Annu. Conf. Eng. Medicine Biol. (EMBC)*, Shanghai, China, Sep. 2005, #340, in CD-ROM.